Polymeric Carbon Nanocomposites from Carbon Nanotubes Functionalized with Matrix Polymer

Yi Lin,[†] Bing Zhou,[†] K. A. Shiral Fernando,[†] Ping Liu,[†] Lawrence F. Allard,[‡] and Ya-Ping Sun*,[†]

Department of Chemistry and Center for Advanced Engineering Fibers and Films, Howard L. Hunter Chemistry Laboratory, Clemson University, Clemson, South Carolina 29634-0973, and High Temperature Materials Laboratory, Oak Ridge National Laboratory, Oak Ridge, Tennessee 37831-6062

Received June 27, 2003; Revised Manuscript Received July 29, 2003

ABSTRACT: Single-walled and multiple-walled carbon nanotubes were functionalized with poly(vinyl alcohol) (PVA) in esterification reactions. Similar to the parent PVA, the functionalized carbon nanotube samples are soluble in highly polar solvents such as DMSO and water. The common solubilities have allowed the intimate mixing of the functionalized nanotubes with the matrix polymer for the wet-casting of nanocomposite thin films. The PVA−carbon nanotube composite films are of high optical quality, without any observable phase separation, and the carbon nanotubes in the films are as well-dispersed as in solution. The functionalization of carbon nanotubes by the matrix polymer is apparently an effective way in the homogeneous nanotube dispersion for high-quality polymeric carbon nanocomposite materials. Results from characterizations of the solubilized carbon nanotubes and the nanocomposite thin films are presented and discussed.

Introduction

Many potential applications of polymer−carbon nanotube composite materials have been proposed and discussed.[1−8] Significant efforts have been made in the fabrication of these nanocomposites by dispersing either single-walled (SWNT) or multiple-walled (MWNT) carbon nanotubes into various polymer matrices. For example, carbon nanotubes have been dispersed into matrices of conjugated polymers, such as poly(phenylenevinylene) (PPV) and derivatives, to prepare composites of interesting optoelectronic properties.[3,4] Carbon nanotubes have also been used as fillers in epoxy resin to take advantage of their superior mechanical properties.[2] Solution-phase processing has been a commonly used method in the dispersion of carbon nanotubes and the subsequent fabrication of the nanocomposites.[4−8] However, carbon nanotubes are insoluble and bundled, which makes their homogeneous dispersion in hosting polymer matrices a significant challenge. Among more successful approaches for the dispersion include the sonication of carbon nanotubes in the presence of polymers, such as PPV derivatives,[4,5] poly(vinylpyrrolidone),[9] and starch,[10] and the in situ polymerization of monomers in the presence of carbon nanotubes.[11,12]

It is now well established that carbon nanotubes can be solubilized through chemical modification or functionalization.[13−15] Two different approaches for chemical modification on carbon nanotube surface have been developed: addition to the nanotube wall[15−17] and functionalization at defect sites.[18−23] The latter typically takes advantage of the carboxylic acid moieties at the defect sites to link polymeric and oligomeric functional groups. There have already been strong experimental evidence for the existence of nanotube-bound carboxylic acids and also evidence showing that reactions targeting the carboxylic acids result in the solubilization of the nanotubes.[13,24] The solubilized carbon nanotubes, especially those from the polymer functionalization, are important to the preparation of polymeric carbon nanocomposites.[7,8,22a,25,26] For example, Grady and co-workers fabricated polypropylene−carbon nanotube composites by dispersing octadecylamine-functionalized SWNTs into the polymer matrix via a solution-based method to take advantage of the common solubility of the functionalized nanotube sample and the matrix polymer in the same selected solvent.[25] Sun and co-workers solubilized carbon nanotubes through the covalent attachment of polystyrene copolymers and then dispersed the polystyrene copolymer-functionalized carbon nanotubes into the polystyrene matrix for the fabrication of nanocomposite thin films.[8] Krishnamoorti, Tour, and co-workers reported that functionalized SWNTs could also be used in the polystyrene−carbon nanotube composites for melt-state rheology studies.[7]

The use of polymers that are structurally close to the matrix polymer for the functionalization of carbon nanotubes is obviously a desirable approach in the development of polymeric carbon nanocomposites. It ensures compatibility of the functionalized carbon nanotubes with the polymer matrix to avoid any potential microscopic phase separation in the nanocomposites. Generally speaking, the species used in the functionalization and solubilization of carbon nanotubes become "impurities" in the final nanocomposites. Also considered as impurities are some units in the polymers that are structurally close to the matrix polymer, such as the derivatized styrene units in the polystyrene copolymers.[8] Thus, an ideal polymeric carbon nanocomposite may be prepared by using solubilized carbon nanotubes that are functionalized with the matrix polymer. One of the polymer systems that can be used for such a purpose is poly(vinyl alcohol) (PVA). PVA is an excellent matrix polymer for nanocomposites, forming thin films of high optical quality in wet-casting. In fact, PVA thin

[†] Clemson University.
[‡] Oak Ridge National Laboratory.
* Corresponding author.

10.1021/ma0348876 CCC: $25.00
Published on Web 08/23/2003

film has commonly been employed as a polymer host for a variety of chromophores in optical spectroscopic investigations.[27]

In this paper, we report the solubilization of both SWNTs and MWNTs via the functionalization with PVA. Similar to the parent polymer, the functionalized nanotube samples are soluble in highly polar solvents such as DMSO and water. The solubility has allowed the casting of high-quality PVA−carbon nanotube composite thin films from aqueous solutions. Results from characterizations of the solubilized carbon nanotubes and the nanocomposite thin films are presented and discussed.

Experimental Section

Materials. PVA ($M_W \sim 70\,000-100\,000$, 99% hydrolyzed) was purchased from Alfa Aesar. *N,N′*-Dicyclohexylcarbodiimide (DCC, 99%) and 4-(dimethylamino)pyridine (DMAP, 99%) were obtained from Acros, and 1-hydroxybenzotriazole (HOBT, containing less than 5% H_2O) and trifluoroacetic acid (TFA, 99%) were from Aldrich. Dimethyl sulfoxide (DMSO, 99.5%) and *N,N′*-dimethylformamide (DMF, 99%) were purchased from Burdick & Jackson and Acros, respectively, and dried over molecular sieves before use. Deuterated water and DMSO for NMR measurements were obtained from Cambridge Isotope Laboratories. Dialysis membranes were supplied by Spectrum Laboratories.

Measurements. UV/vis/NIR absorption spectra were recorded on Shimadzu UV2101PC and UV3100 and Thermo-Nicolet Nexus 670 FT−near-IR spectrometers. Raman spectra were obtained on a Renishaw Raman spectrometer equipped with a 50 mW diode laser source for 780 nm excitation and a CCD detector. NMR measurements were performed on a JEOL Eclipse +500 NMR spectrometer. Thermal gravimetric analysis (TGA) was carried out on a Mettler-Toledo TGA/SDTA851e system. Scanning electron microscopy (SEM) images were obtained on a Hitachi S4700 field-emission SEM system. Transmission electron microscopy (TEM) analyses were conducted on Hitachi H-7000 (100 kV) and Hitachi HF-2000 (200 kV) TEM systems equipped with a Gatan AccuView camera (model 789) and a Gatan Multi-Scan CCD camera, respectively, for digital imaging. Ultrathin cross-sectional slices of the nanocomposite films for TEM imaging were obtained using an Ultracut-E microtomy system equipped with a diamond knife.

Carbon Nanotubes and Functionalization. The SWNT and MWNT samples were produced in Professor A. M. Rao's laboratory (Department of Physics and Astronomy, Clemson University) using the arc-discharge method and the chemical vapor deposition (CVD) method, respectively.[28] In the purification of SWNTs, an as-prepared sample (4 g) was suspended in an aqueous HNO_3 solution (2.6 M, 800 mL) and refluxed for 48 h. Upon centrifuging to remove the supernatant, the remaining solid sample was washed repeatedly with deionized water and then resuspended in an aqueous buffer (pH = 10) containing surfactant Triton X100 (10 mL in 600 mL buffer solution). The suspension was passed through a 200 nm membrane cartridge in a cross-flow filtration system (Spectrum MiniKros Lab). Additional aqueous buffer (pH = 10, 15 L) and deionized water (pH = 7, 7 L), both containing Triton X100 (0.2% in volume), were used as eluents. The permeation flow rate was controlled at ~70 mL/min. The remaining materials in the processing reservoir were collected. After thoroughly washed with methanol and toluene to remove the surfactant, the solid sample was suspended in concentrated HCl solution (37%) and refluxed for 24 h, followed by centrifuging, repeated washing with deionized water, and drying under vacuum to yield purified SWNTs (877 mg).

The CVD-produced MWNT samples were known to contain considerably less carbon nanoparticles and impurities. Thus, the purification was primarily to remove iron-containing catalysts. The as-prepared MWNT sample was suspended in an aqueous HNO_3 solution (2.6 M) and refluxed for 48 h, followed by centrifuging, repeated washing with deionized water, and drying under vacuum.[20b]

Scheme 1

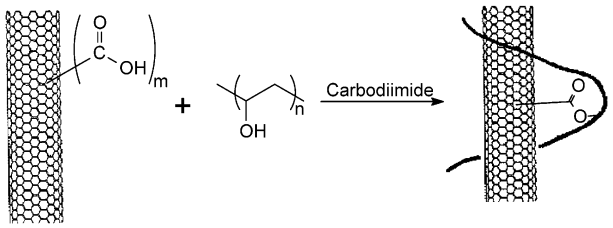

Both SWNTs and MWNTs were functionalized with PVA in carbodiimide-activated esterification reactions (Scheme 1).[20c] In a typical reaction, DCC (400 mg, 1.2 mmol), DMAP (66 mg, 0.3 mmol), and HOBT (130 mg, 0.6 mmol) were dissolved in DMSO (15 mL). A purified SWNT sample (166 mg) was added to the solution, followed by sonication for 1 h. Then, a solution of PVA in DMSO (166 mg/mL, 10 mL) was added, and the mixture was sonicated for another 24 h. The dark suspension thus obtained was centrifuged at a high speed (7200 rpm). The supernatant was a dark-colored solution of the functionalized SWNTs. Upon the removal of solvent, the black solid sample was first washed thoroughly with acetone and then dissolved in water with some heating. The aqueous solution was placed in a dialysis tubing (cutoff molecular weight ~ 100 000) for dialysis against fresh deionized water for 3 days. Upon the complete removal of water, a black glassy sample of PVA-functionalized SWNTs (340 mg) was obtained.

The same procedure was applied to obtain the PVA-functionalized MWNT sample also as black glassy solids.

Results and Discussion

The functionalization reaction was evaluated in terms of the mass balance to determine the amount of carbon nanotubes being solubilized in the reaction. Since the solid residue from the functionalization reaction contained partially functionalized carbon nanotubes (but not sufficient to become soluble),[13a] the mass balance calculation was corrected for the amount of PVA trapped in the solid residue via TGA analyses. For both SWNTs and MWNTs, about 40% of the starting nanotube sample was solubilized in the functionalization reaction with PVA.

Functionalized Carbon Nanotubes. The PVA-functionalized carbon nanotubes are soluble in water and DMSO with the aid of moderate heating, similar to the parent PVA. The dark-colored solutions from the soluble samples are stable, without any precipitations over time. Shown in Figure 1 is the UV/vis/NIR absorption spectrum of the PVA-functionalized SWNTs. The spectrum over the UV/vis regions is essentially a featureless curve, typical of functionalized carbon nanotubes with various other functional groups.[13a] The near-IR region is featured by two broad bands centered at ~1870 nm (5350 cm^{-1} or 0.66 eV) and ~1050 nm (9520 cm^{-1} or 1.19 eV), which may be assigned to the first and second pairs of van Hove singularities in the electronic density of states for semiconducting SWNTs, respectively.[29] These transitions in the NIR region are typical of SWNTs produced by the arc-discharge method,[29] suggesting that not only are there abundant SWNTs in the soluble sample but also the electronic structures of the SWNTs are largely preserved after the functionalization with PVA.

The samples for TEM analyses were prepared by placing a few drops of a PVA-functionalized carbon nanotube solution onto carbon-coated or holey carbon-coated copper grid, followed by evaporation of the

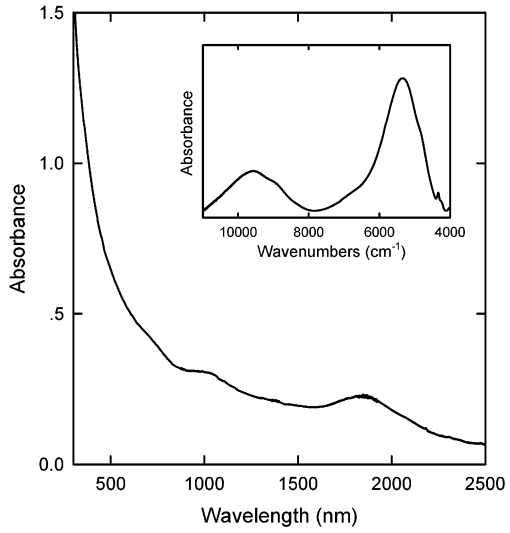

Figure 1. UV/vis/NIR spectrum (recorded on a Shimadzu UV3100 spectrophotometer) of PVA-functionalized SWNTs on a glass substrate. Shown in the inset is the NIR spectrum (recorded on Nexus 670 FT-NIR spectrometer) of the same sample after the subtraction of a sloped baseline.

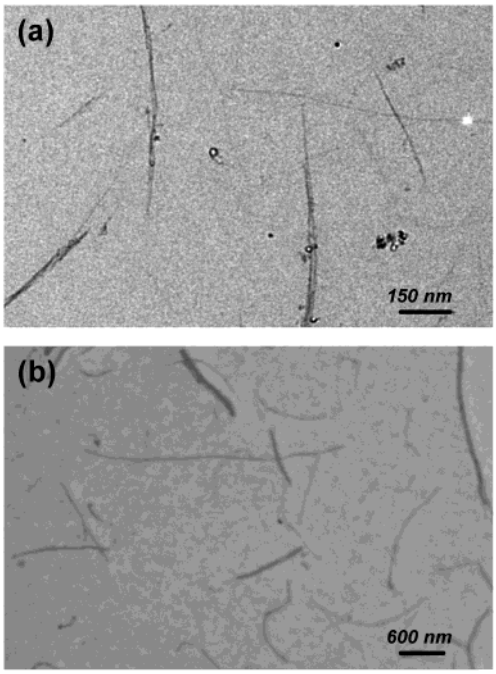

Figure 2. Typical TEM images of (a) PVA-functionalized SWNTs and (b) PVA-functionalized MWNTs.

solvent. The TEM images in Figure 2 show the functionalized SWNTs and MWNTs. These nanotubes appear relatively shorter than those in the starting samples, probably due to the shortening effect associated with the prolonged sonication in the carbodiimide activation.[20c] At a high resolution for SWNTs lying across holes on the holey carbon grid (Figure 3), the image shows that the nanotube surface is covered by amorphous materials, which are likely the attached PVA polymers.[30] There were probably also polymer−polymer interactions during the solvent evaporation in the TEM sample preparation, resulting in the aggregation of several PVA-functionalized SWNTs. Some of the polymer coverage of the nanotube surface could be removed in an ex situ thermal treatment prior to the TEM imaging.[30] In the experiment, the PVA-functionalized SWNT sample was deposited on a holey $LaCrO_3$-coated stainless steel grid. After the specimen was heated at 370 °C in air for 30 min, the nanotube surface became relatively cleaner according to the results from TEM imaging.

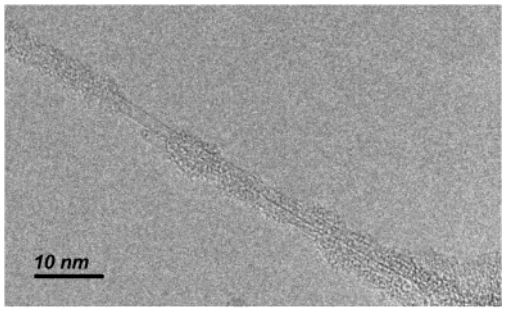

Figure 3. A high-resolution TEM image of PVA-functionalized SWNTs.

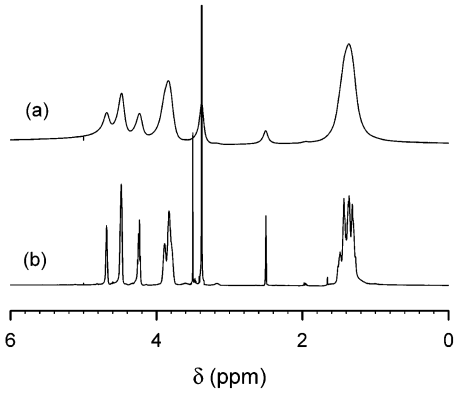

Figure 4. ^{1}H NMR spectra of neat PVA (bottom) and PVA-functionalized SWNTs (top) in room temperature DMSO-d_6.

The solubility of the PVA-functionalized carbon nanotubes allowed solution-phase NMR characterization. For example, the ^{1}H NMR spectrum of the soluble SWNT sample in DMSO-d_6 is compared with that of neat PVA in Figure 4. The latter exhibits the polymer backbone signals at 3.95−3.75 ppm ($CH_2C\mathbf{H}OH$) and 1.6−1.2 ppm ($C\mathbf{H_2}CHOH$) and the hydroxyl signals at 5−4 ppm, from which the stereoregularity of PVA is estimated as isotactic:heterotactic:syndiotactic of roughly 2:5:3.[31] Upon the attachment to SWNTs the PVA proton signals become much broadened but maintain similar chemical shifts (Figure 4). The ^{13}C NMR spectrum of the PVA-functionalized SWNT sample is similar to that of the neat PVA. The absence of ^{13}C signals for the ester linkages could be due to the relatively low concentrations of those carbons in the NMR sample.

The presumed presence of ester linkages in the PVA-functionalized carbon nanotubes was evaluated indirectly in terms of chemical defunctionalization under hydrolysis conditions amenable to the dissociation of the ester bonds.[21] In an acid-catalyzed hydrolysis reaction, TFA was added to an aqueous solution of the PVA-functionalized SWNTs, and the mixture was stirred at room temperature. There was the formation of suspended black solids in the reaction, which were recovered via high-speed centrifuging. The SEM image of the solid sample shows a composite-like material of a high SWNT content (Figure 5). It is possible that in the chemical defunctionalization precipitation may have occurred after only a partial ester cleavage, which prevents the further effective removal of functional groups for a complete defunctionalization.

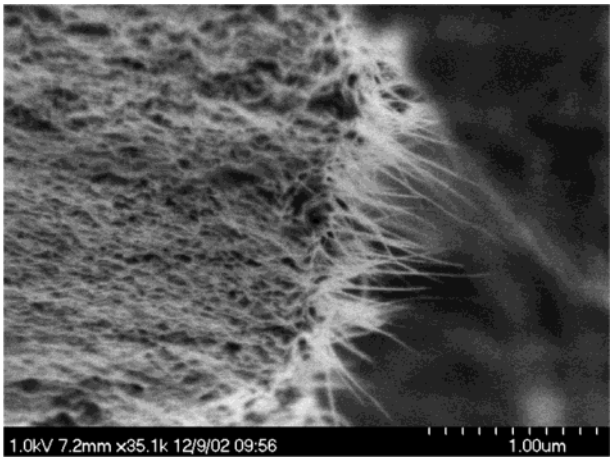

Figure 5. SEM image of the dark precipitates from the chemical defunctionalization reaction of PVA-functionalized SWNTs.

Nanocomposites. PVA is an excellent hosting polymer matrix for optically high-quality composite films.[27] The solubilization of carbon nanotubes by the functionalization with the matrix polymer PVA should in principle allow the fabrication of "ideal" polymer−carbon nanocomposite materials (free from any "impurities", such as the species or groups required for the functionalization of carbon nanotubes in other polymer systems).[7,8,25]

A typical procedure for the wet-casting of a PVA−nanotube composite thin film is to mix an aqueous solution of PVA-functionalized carbon nanotubes with a highly viscous aqueous solution of PVA. The mixture was first sonicated for a short period of time and then stirred for 4−12 h until homogeneous and visually without any air bubbles. The viscous but homogeneous solution was then dropped onto a glass substrate for film-casting with an adjustable film applicator (from Gardco). The thin film on the substrate was dried at room temperature for 24 h and then peeled off to be free-standing. The PVA−nanotube composite films prepared in this study were typically 15 mm × 30 mm in size and 50−200 μm in thickness.

The PVA−nanotube composite thin films were of high optical quality, transparent, and homogeneous. The film color was dependent on the nanotube loading. Shown in Figure 6 are the UV/vis/NIR absorption spectra of the films (thickness ∼ 100 μm) with different SWNT loadings of approximately 0.1, 0.5, and 1 wt %. The nanotube contents in the films were estimated in terms of mass balance calculations from the known nanotube contents in the PVA-functionalized nanotube samples, which were determined in TGA analyses.[32] The UV/vis portion of the spectrum is similar to that of the PVA-functionalized SWNTs in solution. The near-IR absorption spectrum is also characterized by the two broad transitions, similar to those in Figure 1. The absorption properties of the nanocomposite films suggest that the carbon nanotubes embedded in the films are practically the same as those in the PVA-functionalized carbon nanotube samples. The dependence of the absorption on the nanotube loading appears to follow the Lambert−Beer law (Figure 6, inset).

The PVA−SWNT nanocomposite films were characterized by Raman spectroscopy. As shown in Figure 7, the Raman spectra of the films exhibit the characteristic nanotube features on top of a broad luminescence

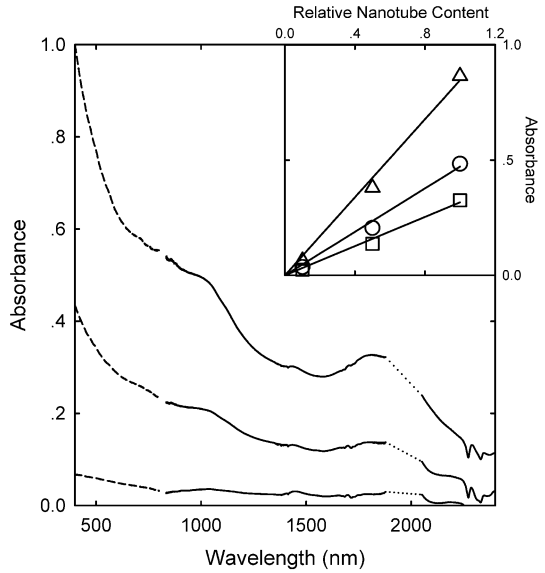

Figure 6. Absorption spectra of PVA−SWNT composite films of different SWNT contents. The inset shows the dependencies of absorbance at 450 (△), 1038 (○), and 1839 nm (□) on nanotube contents in the composite films.

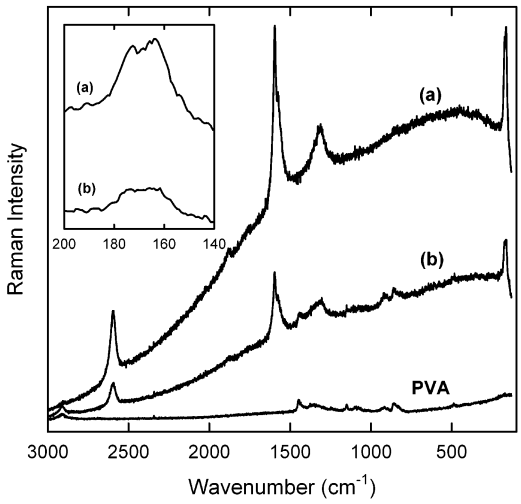

Figure 7. Raman spectra of PVA−SWNT composite films with SWNT contents of (a) 2.5% and (b) 0.5% and the neat PVA film. The luminescence interference may be considered as an indication that the nanotubes are well-dispersed with surface passivation, as discussed in ref 13a.

background, with the D*-band at ∼2595 cm^{-1}, G-band at ∼1595 cm^{-1}, D-band at ∼1310 cm^{-1}, and the radial breathing mode at ∼170 cm^{-1} (Figure 7, inset). Apparently, the peak intensities are higher for composite films with higher nanotube loadings. There were reports that some Raman features of SWNTs might shift to higher frequencies upon their being incorporated into a polymeric matrix via a dispersion-curing procedure.[2b,33] The shifts were attributed to hydrostatic compression to the nanotube bundles. However, such resonance shifts are absent in the Raman spectra of the PVA−SWNT nanocomposite films.

To examine the nanotube dispersion in the polymer matrix at the nanoscale, a PVA−MWNT thin film (MWNT content ∼ 3 wt %) was sliced into specimens of ∼100 nm in thickness by microtomy and then analyzed by TEM. As shown in Figure 8, there are obviously abundant MWNTs randomly dispersed in the polymer matrix. In fact, the TEM image is similar to that of the

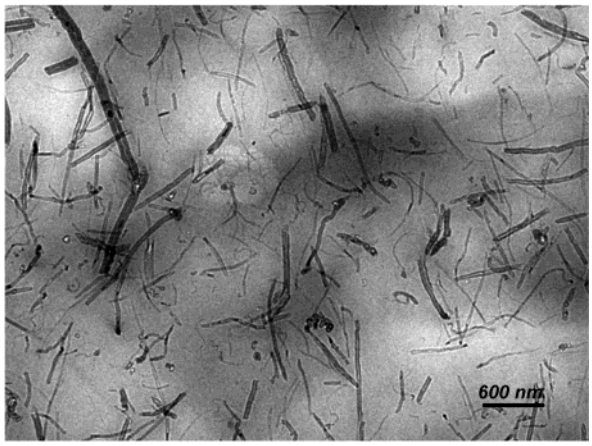

Figure 8. Typical TEM image of a specimen from the cross-sectional microtomy of a PVA−MWNT composite film.

specimen prepared from a PVA-functionalized MWNT solution sample (Figure 2b). For PVA−SWNT composite films, the TEM analysis of the ultrathin slices from microtomy is hindered by a lack of sufficient contrast between the well-dispersed PVA-functionalized SWNTs and the matrix PVA background. Additional experimental effort is needed for the characterization.

In summary, SWNTs and MWNTs can be functionalized by PVA in carbodiimide-activated esterification reactions. The PVA-functionalized carbon nanotubes are soluble in the same solvent for neat PVA, thus allowing the intimate mixing of the nanotubes with the matrix polymer for the wet-casting of nanocomposite thin films. The PVA−carbon nanotubes composite films are of high optical quality, without any observable phase separation. Results from the characterization of the nanocomposite films show that the dispersion of carbon nanotubes is as homogeneous as that in solution. This work demonstrates that the functionalization of carbon nanotubes by the matrix polymer is an effective way in the homogeneous nanotube dispersion for high-quality polymeric carbon nanocomposite materials.

Acknowledgment. We thank Prof. A. M. Rao and his students for supplying the carbon nanotube samples and NSF, NASA, and the Center for Advanced Engineering Fibers and Films (NSF-ERC at Clemson University) for financial support. We also thank the Assistant Secretary for Energy Efficiency and Renewable Energy, Office of Transportation Technologies, as part of the HTML User Program, managed by UT-Battle LLC for DOE (DE-AC05-00OR22725).

References and Notes

(1) (a) Ajayan, P. M. *Chem. Rev.* **1999**, *99*, 1787. (b) Ajayan, P. M.; Zhou, O. Z. *Top. Appl. Phys.* **2001**, *80*, 391.
(2) (a) Ajayan, P. M.; Stephan, O.; Colliex, C.; Trauth, D. *Science* **1994**, *265*, 1212. (b) Ajayan, P. M.; Schadler, L. S.; Giannaris, C.; Rubio, A. *Adv. Mater.* **2000**, *12*, 750.
(3) Ago, H.; Petritsch, K.; Shaffer, M. S. P.; Windle, A. H.; Friend, R. H. *Adv. Mater.* **1999**, *11*, 1281.
(4) (a) Dalton, A. B.; Stephan, C.; Coleman, J. N.; McCarthy, B.; Ajayan, P. M.; Lefrant, S.; Bernier, P.; Blau, W. J.; Byrne, H. J. *J. Phys. Chem. B* **2000**, *104*, 10012. (b) McCarthy, B.; Coleman, J. N.; Czerw, R.; Dalton, A. B.; in het Panhuis, M.; Maiti, A.; Drury, A.; Bernier, P.; Nagy, J. B.; Lahr, B.; Byrne, H. J.; Carroll, D. L.; Blau, W. J. *J. Phys. Chem. B* **2002**, *106*, 2210.
(5) (a) Star, A.; Stoddart, J. F.; Diehl, M.; Boukai, A.; Wong, E. W.; Yang, X.; Chung, S. W.; Choi, H.; Heath, J. R. *Angew. Chem., Int. Ed.* **2001**, *40*, 1721. (b) Steuerman, D. W.; Star, A.; Narizzano, R.; Choi, H.; Ries, R. S.; Nicolini, C.; Stoddart, J. F.; Heath, J. R. *J. Phys. Chem. B* **2002**, *106*, 3124. (c) Star, A.; Liu, Y.; Grant, K.; Ridvan, L.; Stoddart, J. F.; Steuerman, D. W.; Diehl, M. R.; Boukai, A.; Heath, J. R. *Macromolecules* **2003**, *36*, 553.
(6) (a) Qian, D.; Dickey, E. C.; Andrews, R.; Rantell, T. *Appl. Phys. Lett.* **2000**, *76*, 2868. (b) Grimes, C. A.; Dickey, E. C.; Mungle, C.; Ong, K. G.; Qian, D. *J. Appl. Phys.* **2001**, *90*, 4134.
(7) Mitchell, C. A.; Bahr, J. L.; Arepalli, S.; Tour, J. M.; Krishnamoorti, R. *Macromolecules* **2002**, *35*, 8825.
(8) (a) Hill, D. E.; Lin, Y.; Rao, A. M.; Allard, L. F.; Sun, Y.-P. *Macromolecules* **2002**, *35*, 9466. (b) Hill, D. E.; Lin, Y.; Allard, L. F.; Sun, Y.-P. *Int. J. Nanosci.* **2002**, *1*, 213.
(9) O'Connell, M. J.; Boul. P.; Ericson, L. M.; Huffman, C.; Wang, Y. H.; Haroz, E.; Kuper, C.; Tour, J.; Ausman, K. D.; Smalley, R. E. *Chem. Phys. Lett.* **2001**, *342*, 265.
(10) Star, A.; Steuerman, D. W.; Heath, J. R.; Stoddar, J. F. *Angew. Chem., Int. Ed.* **2002**, *41*, 2508.
(11) Tang, B. Z.; Xu, H. *Macromolecules* **1999**, *32*, 2569.
(12) (a) Cochet, M.; Maser, W. K.; Benito, A. M.; Callejas, M. A.; Martinez, M. T.; Benoit, J.-M.; Schreiber, J.; Chauvet, O. *Chem. Commun.* **2001**, 1450. (b) Barraza, H. J.; Pompeo, F.; O'Rear, E. A.; Resasco, D. E. *Nano Lett.* **2002**, *2*, 797. (c) Shaffer, M. S. P.; Koziol, K. *Chem. Commun.* **2002**, 2074. (d) Kumar, S.; Dang, T. D.; Arnold, F. E.; Bhattacharyya, A. R.; Min, B. G.; Zhang, X.; Vaia, R. A.; Park, C.; Adams, W. W.; Hauge, R. H.; Smalley, R. E.; Ramesh, S.; Willis, P. A. *Macromolecules* **2002**, *35*, 9039.
(13) (a) Sun, Y.-P.; Fu, K.; Lin, Y.; Huang, W. *Acc. Chem. Res.* **2002**, *35*, 1096. (b) Niyogi, S.; Hamon, M. A.; Hu, H.; Zhao, B.; Bhowmik, P.; Sen, R.; Itkis, M. E.; Haddon, R. C. *Acc. Chem. Res.* **2002**, *35*, 1105.
(14) (a) Bahr, J. L.; Tour, J. M. *J. Mater. Chem.* **2002**, *12*, 1952. (b) Hirsch, A. *Angew. Chem., Int. Ed.* **2002**, *41*, 1853.
(15) Khabashesku, V. N.; Billups, W. E.; Margrave, J. L. *Acc. Chem. Res.* **2002**, *35*, 1087 and references therein.
(16) Dyke, C. A.; Tour, J. M. *J. Am. Chem. Soc.* **2003**, *125*, 1156.
(17) Saini, R. K.; Chiang, I. W.; Peng, H.; Smalley, R. E.; Billups, W. E.; Hauge, R. H.; Margrave, J. L. *J. Am. Chem. Soc.* **2003**, *125*, 3617.
(18) Chen, J.; Hamon, M. A.; Hu, H.; Chen, Y.; Rao, A. M.; Eklund, P. C.; Haddon, R. C. *Science* **1998**, *282*, 98.
(19) (a) Hamon, M. A.; Chen, J.; Hu, H.; Chen, Y.; Itkis, M. E.; Rao, A. M.; Eklund, P. C.; Haddon, R. C. *Adv. Mater.* **1999**, *11*, 834. (b) Chen, J.; Rao, A. M.; Lyuksyutov, S.; Itkis, M. E.; Hamon, M. A.; Hu, H.; Cohn, R. W.; Eklund, P. C.; Colbert, D. T.; Smalley, R. E.; Haddon, R. C. *J. Phys. Chem. B* **2001**, *105*, 2525.
(20) (a) Riggs, J. E.; Guo, Z.; Carroll, D. L.; Sun, Y.-P. *J. Am. Chem. Soc.* **2000**, *122*, 5879. (b) Lin, Y.; Rao, A. M.; Sadanadan, B.; Kenik, E. A.; Sun, Y.-P. *J. Phys. Chem. B* **2002**, *106*, 1294. (c) Huang, W.; Lin, Y.; Taylor, S.; Gaillard, J.; Rao, A. M.; Sun, Y.-P. *Nano Lett.* **2002**, *2*, 231.
(21) (a) Sun, Y.-P.; Huang, W.; Lin, Y.; Fu, K.; Kitaygorodskiy, A.; Riddle, L. A.; Yu, Y. J.; Carroll, D. L. *Chem. Mater.* **2001**, *13*, 2864. (b) Fu, K.; Huang, W.; Lin, Y.; Riddle, L. A.; Carroll, D. L.; Sun, Y.-P. *Nano Lett.* **2001**, *1*, 439.
(22) (a) Jin, Z.; Sun, X.; Xu, G.; Goh, S. H.; Ji, W. *Chem. Phys. Lett.* **2000**, *318*, 505. (b) Sano, M.; Kamino, A.; Okamura, J.; Shinkai, S. *Langmuir* **2001**, *17*, 5125.
(23) Banerjee, S.; Wong, S. S. *J. Am. Chem. Soc.* **2002**, *124*, 8940.
(24) (a) Hu, H.; Bhowmik, P.; Zhao, B.; Hamon, M. A.; Itkis, M. E.; Haddon, R. C. *Chem. Phys. Lett.* **2001**, *345*, 25. (b) Mawhinney, D. B.; Naumenko, V.; Kuznetsova, A.; Yates Jr., J. T.; Liu, J.; Smalley, R. E. *Chem. Phys. Lett.* **2000**, *324*, 13.
(25) Grady, B. P.; Pompeo, F.; Shambaugh, R. L.; Resasco, D. E. *J. Phys. Chem. B* **2002**, *106*, 5852.
(26) Sun, Y.-P.; Zhou, B.; Henbest, K.; Fu, K.; Huang, W.; Lin, Y.; Taylor, S.; Carroll, D. L. *Chem. Phys. Lett.* **2002**, *351*, 349.
(27) Lakowicz, R. J. *Principles of Fluorescence Spectroscopy*, 2nd ed.; Plenum Publisher: New York, 1999.
(28) (a) Journet, C.; Maser, W. K.; Bernier, P.; Loiseau, A.; de la Chapelle, M. L.; Lefrant, S.; Deniard, P.; Lee, R.; Fischer, J. E. *Nature (London)* **1997**, *388*, 756. (b) Andrews, R.; Jacques, D.; Rao, A. M.; Derbyshire, F.; Qian, D.; Fan, X.; Dickey, E. C.; Chen, J. *Chem. Phys. Lett.* **1999**, *303*, 467. (c) Rao, A. M.; Jacques, D.; Haddon, R. C.; Zhu, W.; Bower, C.; Jin, S. *Appl. Phys. Lett.* **2000**, *76*, 3813.

(29) Hamon, M. A.; Itkis, M. E.; Niyogi, S.; Alvaraez, T.; Kuper, C.; Menon, M.; Haddon, R. C. *J. Am. Chem. Soc.* **2001**, *123*, 11292.
(30) Lin, Y.; Hill, D. E.; Bentley, J.; Allard, L. F.; Sun, Y.-P. *J. Phys. Chem. B* **2003**, in press.
(31) (a) Moritani, T.; Kuruma, I.; Shibatani, K.; Fujiwara, Y. *Macromolecules* **1972**, *5*, 577. (b) Wu, T. K.; Ovenall, D. W. *Macromolecules* **1973**, *6*, 582.
(32) The typical nanotube content in the PVA-functionalized SWNT samples was about 10% w/w, estimated in terms of TGA analyses (10 °C/min to 800 °C in a N_2 atmosphere), corresponding to an estimated degree of functionalization on the order of 1 PVA chain per 1000 nanotube carbons.
(33) Lourie, O.; Wagner, H. D. *J. Mater. Res.* **1998**, *13*, 2418.

MA0348876